

# Neutrino and axion hot dark matter bounds after WMAP-7

Steen Hannestad<sup>1</sup>, Alessandro Mirizzi<sup>2</sup>, Georg G. Raffelt<sup>3</sup> and Yvonne Y. Y. Wong<sup>4</sup>

<sup>1</sup> Department of Physics and Astronomy  
University of Aarhus, DK-8000 Aarhus C, Denmark

<sup>2</sup> II. Institut für Theoretische Physik, Universität Hamburg  
Luruper Chaussee 149, D-22761 Hamburg, Germany

<sup>3</sup> Max-Planck-Institut für Physik (Werner-Heisenberg-Institut)  
Föhringer Ring 6, D-80805 München, Germany

<sup>4</sup> Institut für Theoretische Teilchenphysik und Kosmologie  
RWTH Aachen, D-52056 Aachen, Germany

E-mail: sth@phys.au.dk, alessandro.mirizzi@desy.de,  
raffelt@mppmu.mpg.de, yvonne.wong@physik.rwth-aachen.de

**Abstract.** We update cosmological hot dark matter constraints on neutrinos and hadronic axions. Our most restrictive limits use 7-year data from the Wilkinson Microwave Anisotropy Probe for the cosmic microwave background anisotropies, the halo power spectrum (HPS) from the 7th data release of the Sloan Digital Sky Survey, and the Hubble constant from Hubble Space Telescope observations. We find 95% CL upper limits of  $\sum m_\nu < 0.44$  eV (no axions),  $m_a < 0.91$  eV (assuming  $\sum m_\nu = 0$ ), and  $\sum m_\nu < 0.41$  eV and  $m_a < 0.72$  eV for two hot dark matter components after marginalising over the respective other mass. CMB data alone yield  $\sum m_\nu < 1.19$  eV (no axions), while for axions the HPS is crucial for deriving  $m_a$  constraints. This difference can be traced to the fact that for a given hot dark matter fraction axions are much more massive than neutrinos.

## 1. Introduction

Cosmological large-scale structure data allow for precise estimates for the parameters of minimal or extended cosmological models. These results have ramifications far beyond cosmology itself, notably in the area of neutrino physics. The well-known hot dark matter constraints provide neutrino mass limits that directly impact neutrino mass searches in single [1] and double [2] beta decay experiments. In a series of papers by our collaboration [3–6] and another group [7] this approach was extended to hadronic axions where the resulting mass limits are complementary to solar axion searches by the CAST experiment [8–10] and the Tokyo axion helioscope [11–13]. In the present work, we use the 7-year data release from the Wilkinson Microwave Anisotropy Probe (WMAP) as an opportunity to update these results, and also modify along the way several other input assumptions as detailed in the main text below.

Within standard cosmological assumptions, the neutrino plus antineutrino number density today, summed over all flavours, is  $n_\nu \sim 336 \text{ cm}^{-3}$ . Currently available cosmological data are not yet sensitive enough to resolve the small mass differences measured in oscillation experiments, so all neutrinos are treated as having the same mass  $m_\nu$ , traditionally expressed by the parameter  $\sum m_\nu = 3m_\nu$ . For axions, on the other hand, the freeze-out temperature and therefore the number density  $n_a$  depends on the axion’s interaction rate with pions and nucleons via

$$\begin{aligned} a + \pi &\leftrightarrow \pi + \pi, \\ a + N &\leftrightarrow N + \pi, \end{aligned} \tag{1.1}$$

where the coupling strength is, in turn, proportional to the axion mass  $m_a$  [4, 14, 15]. Figure 1 shows the relation between  $m_a$  and  $n_a$  computed for the thermalisation processes (1.1) based on the original calculations of reference [4]. For small  $m_a$ , the number density is also small, so assuming  $m_a = 0$  implies  $n_a = 0$  which brings us back to standard cosmology. Near the hot dark matter limit of  $m_a \sim 1 \text{ eV}$  one finds a present-day number density of  $n_a \sim 50 \text{ cm}^{-3}$ . Therefore, in the relevant mass range, neutrinos are about 6 times more numerous than axions and one expects a hot dark matter limit on  $m_a$  that is roughly twice that on  $\sum m_\nu$ , in agreement with what we find when we use our full range of input data sets.

In detail, however, the situation is more subtle. Conventional wisdom says that hot dark matter constraints arise primarily from the shape of the measured matter power spectrum, since hot dark matter free-streaming suppresses the growth of matter perturbations and hence the clustering power on small scales. However, recent cosmological data have become so precise that one finds a useful limit on  $\sum m_\nu$  of order 1 eV already from the cosmic microwave background (CMB) anisotropies alone, notably from the increased amplitude of the first acoustic peak in the temperature auto-correlation spectrum due to the early integrated Sachs–Wolfe (ISW) effect [16]. The same is however not true for axion hot dark matter, since for the same hot dark matter fraction, the axion is necessarily some 6 times heavier than the equivalent neutrino. Thus

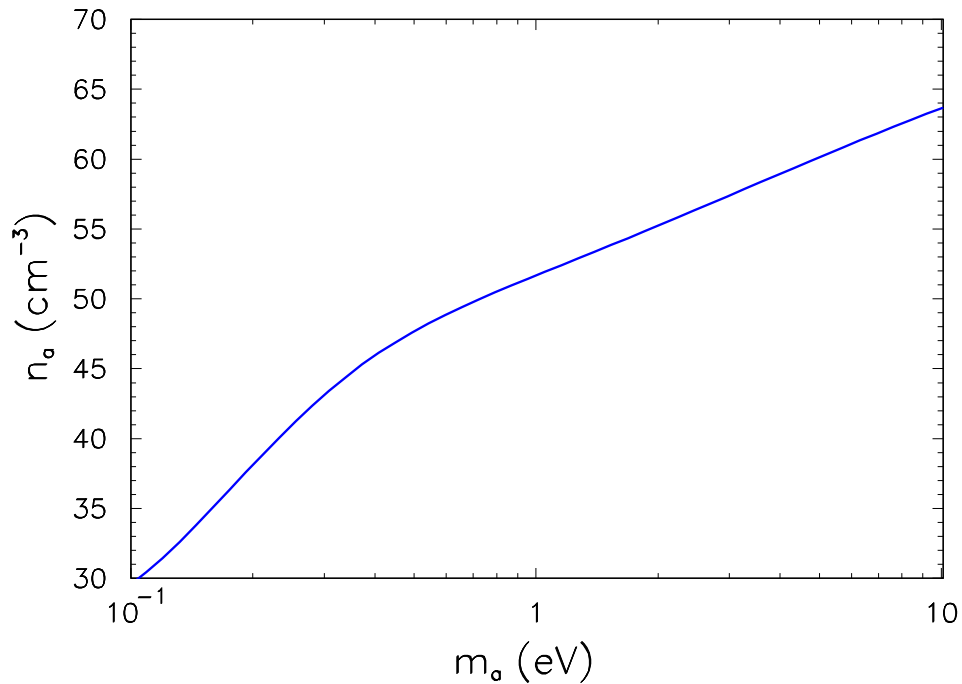


**Figure 1.** Axion number density  $n_a$  as a function of the axion mass  $m_a$  assuming the hadronic thermalisation processes (1.1) based on the calculations of reference [4].

while neutrinos with masses near the hot dark matter limit ( $m_\nu \lesssim 0.3$  eV) essentially act like radiation at CMB decoupling and contribute strongly to the early ISW effect, the equivalent axion is already nonrelativistic and thus indistinguishable from cold dark matter as far as the CMB is concerned. In the latter case, one needs to use the shape of the matter power spectrum from smaller-scale data in order to put any sensible constraint on  $m_a$ .

In order to derive new hot dark matter limits on neutrinos and axions and to explain their differences, we begin in section 2 with a description of our cosmological model and in section 3 of the data sets used. In section 4 we use standard Bayesian techniques to derive credible intervals for  $\sum m_\nu$  and  $m_a$  separately and for a two-component case based on different combinations of data sets. We discuss and summarise our findings in section 5.

## 2. Cosmological model

We consider a cosmological model with vanishing spatial curvature and adiabatic initial conditions, described by eight free parameters,

$$\boldsymbol{\theta} = \{\omega_{\text{cdm}}, \omega_{\text{b}}, H_0, \tau, \ln(10^{10} A_s), n_s, \sum m_\nu, m_a\}. \quad (2.1)$$

Here,  $\omega_{\text{cdm}} = \Omega_{\text{cdm}} h^2$  is the physical cold dark matter density,  $\omega_{\text{b}} = \Omega_{\text{b}} h^2$  the baryon density,  $H_0 = h 100 \text{ km s}^{-1} \text{ Mpc}^{-1}$  the Hubble parameter,  $\tau$  the optical depth to reionisation,  $A_s$  the amplitude of the primordial scalar power spectrum, and  $n_s$  its

**Table 1.** Priors and standard values for the cosmological fit parameters considered in this work. All priors are uniform (top hat) in the given intervals.

| Parameter                   | Standard | Prior     |
|-----------------------------|----------|-----------|
| $\omega_{\text{cdm}}$       | —        | 0.01–0.99 |
| $\omega_{\text{b}}$         | —        | 0.005–0.1 |
| $h$                         | —        | 0.4–1.0   |
| $\tau$                      | —        | 0.01–0.8  |
| $\ln(10^{10} A_{\text{s}})$ | —        | 2.7–4.0   |
| $n_{\text{s}}$              | —        | 0.5–1.5   |
| $\sum m_{\nu}$ [eV]         | 0        | 0–10      |
| $m_{\text{a}}$ [eV]         | 0        | 0–10      |

spectral index. These six parameters represent the simplest parameter set necessary for a consistent interpretation of the currently available data.

In addition, we allow for a nonzero sum of neutrino masses  $\sum m_{\nu}$  and a nonvanishing axion mass  $m_{\text{a}}$ . These extra parameters will be varied one at a time, as well as in combination. Their “standard” values are given in table 1, along with the priors for all cosmological fit parameters considered here.

### 3. Data

#### 3.1. Cosmic microwave background (CMB)

We use a compilation of measurements of the CMB temperature and polarisation anisotropies from WMAP after seven years of observation [17, 18], ACBAR [19], BICEP [20], and QUAD [21].

#### 3.2. Halo power spectrum (HPS)

We use the halo power spectrum constructed from the luminous red galaxy (LRG) sample of the seventh data release of the Sloan Digital Sky Survey (SDSS-DR7) [22]. The full HPS data set consists of 45 data points, covering wavenumbers from  $k_{\text{min}} = 0.02 \text{ hMpc}^{-1}$  to  $k_{\text{max}} = 0.2 \text{ hMpc}^{-1}$ . We fit this data set following the procedure of reference [22], using a properly smeared power spectrum to model nonlinear mode coupling. The smearing procedure requires that we supply a smooth, no-wiggle power spectrum, which we construct using the discrete spectral analysis technique introduced in reference [23].

#### 3.3. Baryon acoustic oscillations (BAO)

The baryon acoustic oscillation scale has been extracted from SDSS-DR7 [24], which provides an angular diameter distance measure at  $z = 0.275$ . However, since parameters like  $\sum m_{\nu}$  and  $m_{\text{a}}$  can in principle affect the acoustic scale, care needs to be taken when

**Table 2.** 1D marginal 95% upper bounds on  $\sum m_\nu$  and  $m_a$  for several different choices of data sets and models.

| Model                       | Data set    | $\sum m_\nu$ [eV] | $m_a$ [eV]    |
|-----------------------------|-------------|-------------------|---------------|
| Fixed $m_a = 0$             | CMB only    | 1.19              | —             |
|                             | CMB+BAO     | 0.85              | —             |
|                             | CMB+HST     | 0.58              | —             |
|                             | CMB+HPS     | 0.61              | —             |
|                             | CMB+HPS+HST | 0.44              | —             |
| Fixed $\sum m_\nu = 0$      | CMB only    | —                 | No constraint |
|                             | CMB+BAO     | —                 | No constraint |
|                             | CMB+HST     | —                 | No constraint |
|                             | CMB+HPS     | —                 | 1.07          |
|                             | CMB+HPS+HST | —                 | 0.91          |
| Free $\sum m_\nu$ and $m_a$ | CMB+HPS     | 0.58              | 0.82          |
|                             | CMB+HPS+HST | 0.41              | 0.72          |

evaluating the BAO likelihood. We refer the reader to reference [23] for a more detailed discussion of this issue.

### 3.4. Hubble parameter from the Hubble Space Telescope (HST)

We adopt the constraint on the Hubble parameter derived from observations with the Hubble Space Telescope [25].

## 4. Results

We use standard Bayesian inference techniques and explore the model parameter space with Monte Carlo Markov Chains (MCMC) generated using the publicly available COSMOMC package [26]. Our results are summarised in table 2 and figure 2.

In agreement with several recent papers, the CMB alone provides a fairly robust limit on  $\sum m_\nu$ . With  $m_a$  held fixed at zero, we find  $\sum m_\nu < 1.2$  eV at 95% C.L. using WMAP and other CMB data, while Komatsu *et al.* find  $\sum m_\nu < 1.3$  eV at 95% C.L. from WMAP alone [18].

It is noteworthy that for the opposite case when  $m_\nu$  is fixed at zero, CMB data provide no constraint on  $m_a$ . At first sight this might seem contradictory, but there is a simple explanation. The suppression of small scale power is essentially controlled by the fraction of hot to cold dark matter,  $f_{\text{hdm}} = \omega_{\text{hdm}}/\omega_{\text{cdm}}$ , for both axions and neutrinos. This can be seen in figure 4 where the red/solid and green/dash lines have the same asymptotic behaviour at large  $k$ . However, the number density of axions is six times smaller than that of neutrinos. Therefore in order to give the same contribution to  $\omega_{\text{hdm}}$ , the mass of the axion must be correspondingly larger than the neutrino mass.

In two examples shown in figures 3 and 4, both the neutrino and the axion hot

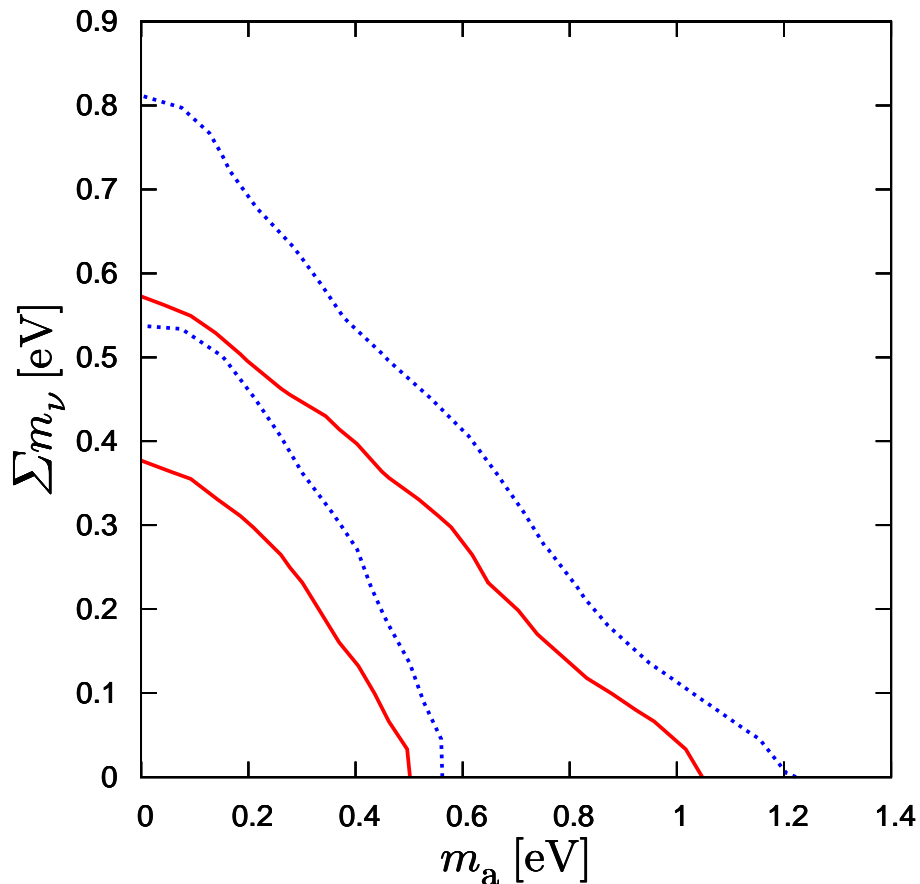


**Figure 2.** 2D marginal 68% and 95% contours in the  $\sum m_\nu - m_a$  plane. The blue lines correspond to our results using CMB+HPS, and the red lines using CMB+HPS+HST.

dark matter models have  $\omega_{\text{hdm}} = 0.013$ , but the corresponding particle masses are  $\sum m_\nu = 1.2$  eV (or  $m_\nu = 0.4$  eV) and  $m_a \simeq 2.4$  eV respectively. The temperature at recombination is approximately 0.2 eV. A neutrino with  $m_\nu = 0.4$  eV would still be semi-relativistic at this time and contribute significantly to the early ISW effect. At  $m_a \simeq 2.4$  eV, however, the axion is nonrelativistic at recombination and behaves more like cold dark matter. This disparity between the two hot dark matter candidates can be clearly seen in figure 3, where the CMB temperature anisotropy spectrum for the axion model is almost indistinguishable from standard  $\Lambda$ CDM, while its neutrino counterpart shows a pronounced early ISW effect.

The same effect is also manifest in the matter power spectrum shown in figure 4, where the epoch of matter–radiation equality—marked by the turning point of the spectrum—is different for axions and neutrinos. In the neutrino case, matter–radiation equality happens later, leading to a turning point at a much smaller value of  $k$  compared with its  $\Lambda$ CDM counterpart. In the axion case, the corresponding matter power spectrum traces closely that of the  $\Lambda$ CDM model up to  $k \sim 0.02 h \text{ Mpc}^{-1}$ . Beyond this point, axion free–streaming sets in and suppresses the power on small scales relative  $\Lambda$ CDM. The amount of suppression in  $P(k)$  at large  $k$  values is similar in both the

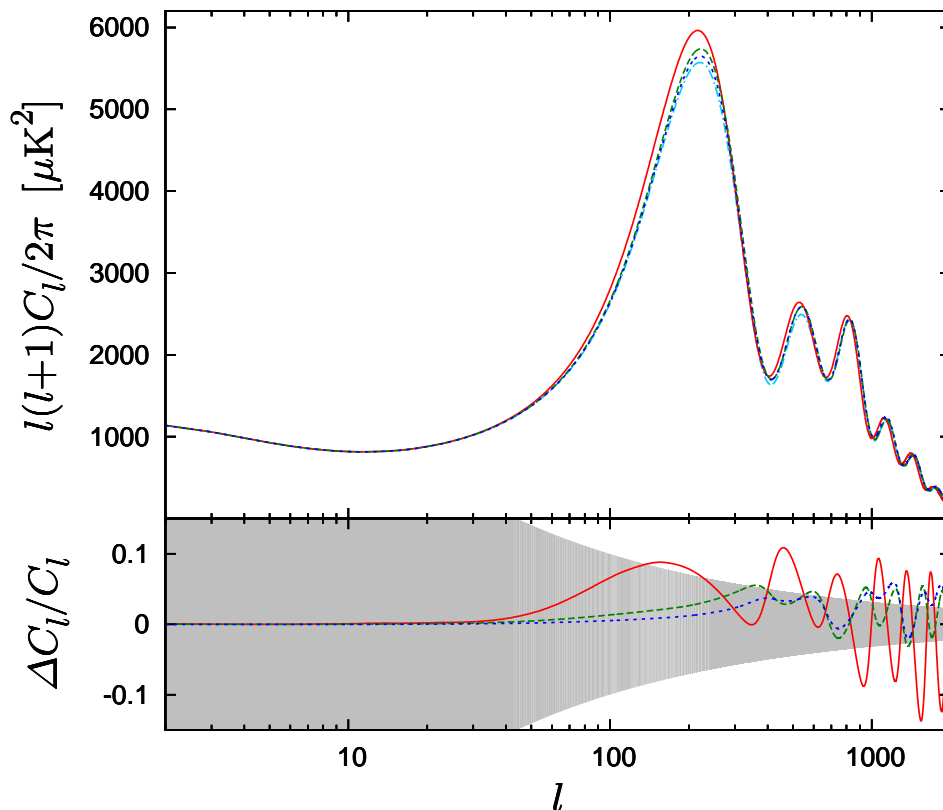


**Figure 3.** CMB temperature anisotropy spectra for various mixtures of cold and hot dark matter, where  $\omega_{\text{cdm}} + \omega_{\nu} + \omega_a = 0.112$  is held constant. Bottom: Differences to standard  $\Lambda\text{CDM}$ ; the shaded/grey area indicates cosmic variance. Light blue/dot-dash line: standard  $\Lambda\text{CDM}$  ( $\omega_{\text{cdm}} = 0.112$ ,  $\omega_a = 0$ ,  $\omega_{\nu} = 0$ ). Red/solid line:  $\Lambda\text{CDM}+\nu$  with  $\sum m_{\nu} = 1.2$  eV ( $\omega_{\text{cdm}} = 0.099$ ,  $\omega_{\nu} = 0.013$ ). Green/dash line:  $\Lambda\text{CDM}+a$  with  $m_a = 2.4$  eV ( $\omega_{\text{cdm}} = 0.099$ ,  $\omega_a = 0.013$ ). Dark blue/dotted line: Extreme axion case with  $m_a = 10$  eV ( $\omega_{\text{cdm}} = 0.0498$ ,  $\omega_a = 0.0622$ ).

neutrino and the axion case as expected, since this is governed primarily by  $f_{\text{hdm}}$ .

Figures 3 and 4 also show an extreme example of power spectra for  $m_a = 10$  eV, corresponding to  $\omega_a = 0.0622$ , actually exceeding  $\omega_{\text{cdm}} = 0.0498$ . Axions with such a large mass act essentially as cold dark matter as far as CMB anisotropies are concerned.

In practice this means that when only CMB data are used, it is difficult to distinguish a several-eV axion model from the standard  $\Lambda\text{CDM}$  model, and accordingly WMAP provides no useful upper bound on  $m_a$ . This is true even when additional priors are imposed, either in the form of the BAO scale, or the HST measurement of the Hubble parameter. Only when low-redshift small-scale data containing *shape* information such as the HPS are added does an upper bound on  $m_a$  emerge. This is an example of the point discussed in reference [23], i.e., that it is crucial to extract the full matter power spectrum from a large scale structure survey because it contains important information not stored in the geometric BAO scale.

From our most restrictive data sets and allowing both the neutrino and the axion masses to vary simultaneously, we find for the axion mass  $m_a < 0.72$  eV (95% C.L.),

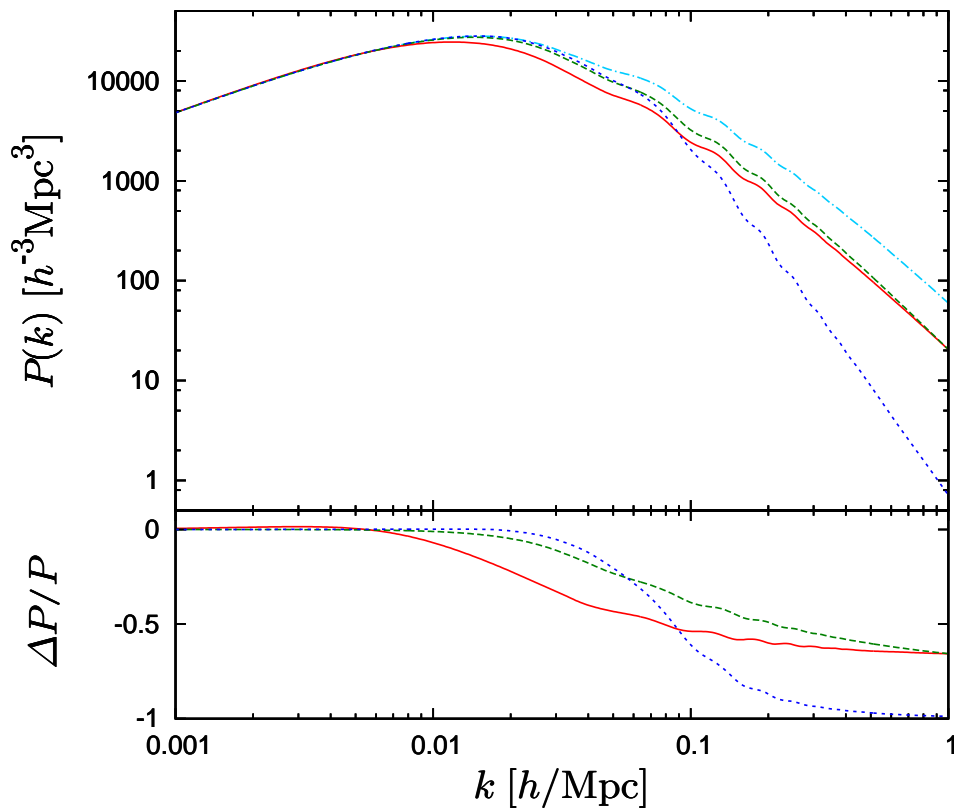


**Figure 4.** Same as figure 3, but for the matter power spectrum.

after marginalising over all other model parameters including  $\sum m_\nu$ . The corresponding 2D marginalised 68% and 95% contours in the  $\sum m_\nu - m_a$  plane are shown in figure 2. This new limit on  $m_a$  is somewhat tighter than our previously published bound of  $m_a < 1.02$  eV (95% C.L.) using the 5-year WMAP data [6]. Fixing  $\sum m_\nu$  to zero, the limit on  $m_a$  becomes less restrictive ( $m_a < 0.91$  eV at 95% C.L.), which would be applicable if future laboratory experiments were to provide a significant constraint on  $m_\nu$ . On the other hand, if these experiments were to measure a value of  $m_\nu$  close to the current cosmological limit, then less room would be left for axion hot dark matter and the limit on  $m_a$  would tighten correspondingly.

## 5. Conclusions

We have provided an updated constraint on axion hot dark matter using new cosmological data, most notably CMB data from the WMAP 7-year data release and the final SDSS-DR7 LRG data. We have also pointed out a qualitative difference between neutrino and axion hot dark matter, in that axion masses in the detectable range are large enough that axions are nonrelativistic at recombination. This means they act almost like cold dark matter as far as CMB is concerned and that current CMB data in itself does not provide a useful limit on the axion mass, even when priors from HST or BAO are imposed. In order to properly constrain  $m_a$  it is necessary to include

information on the shape of the matter power spectrum from, for example, the SDSS halo power spectrum.

An interesting question is whether future CMB data will be sensitive to axion hot dark matter. The Planck mission has an estimated sensitivity of  $\sigma(\sum m_\nu) \sim 0.3\text{--}0.5$  eV [27, 28]. But from figure 3 we can already say that even at high multipoles the effect of axion hot dark matter on the CMB anisotropy spectrum is quite small—generally smaller than the uncertainty due to cosmic variance. This leads to the inevitable conclusion that CMB anisotropy observations will remain poor probes of hot dark matter in the several eV range.

Cosmological bounds on neutrino and axion masses are nicely complementary to experimental searches, but cannot replace them. One caveat concerning our axion results is that we need to assume that the predicted thermal population was actually produced after the QCD epoch. In non-standard cosmologies with low reheating temperature the axion population can be severely suppressed and our bounds would not apply [29]. In other scenarios a significant cosmic background of low-mass axions can be produced that remain relativistic until today and do not form hot dark matter [30]. For neutrinos such caveats are less relevant because their thermalisation epoch is well probed by big-bang nucleosynthesis and the presence of radiation with roughly the right abundance has been confirmed by precision cosmology.

## Acknowledgements

We acknowledge use of computing resources from the Danish Center for Scientific Computing (DCSC). In Munich, partial support by the Deutsche Forschungsgemeinschaft under the grant TR 27 “Neutrinos and beyond” and the Cluster of Excellence “Origin and Structure of the Universe” is acknowledged.

## References

- [1] G. Drexlin, J. Phys. Conf. Ser. **136** (2008) 022031.
- [2] S. Schönert, J. Phys. Conf. Ser. **203** (2010) 012014.
- [3] S. Hannestad and G. G. Raffelt, JCAP **0404** (2004) 008 [hep-ph/0312154].
- [4] S. Hannestad, A. Mirizzi and G. G. Raffelt, JCAP **0507** (2005) 002 [hep-ph/0504059].
- [5] S. Hannestad, A. Mirizzi, G. G. Raffelt and Y. Y. Y. Wong, JCAP **0708** (2007) 015 [arXiv:0706.4198].
- [6] S. Hannestad, A. Mirizzi, G. G. Raffelt and Y. Y. Y. Wong, JCAP **0804** (2008) 019 [arXiv:0803.1585].
- [7] A. Melchiorri, O. Mena and A. Slosar, Phys. Rev. D **76** (2007) 041303 [arXiv:0705.2695].
- [8] K. Zioutas *et al.* (CAST Collaboration), Phys. Rev. Lett. **94** (2005) 121301 [hep-ex/0411033].
- [9] S. Andriamonje *et al.* (CAST Collaboration), JCAP **0704** (2007) 010 [hep-ex/0702006].
- [10] E. Arik *et al.* (CAST Collaboration), JCAP **0902** (2009) 008 [arXiv:0810.4482].
- [11] S. Moriyama, M. Minowa, T. Namba, Y. Inoue, Y. Takasu and A. Yamamoto, Phys. Lett. B **434** (1998) 147 [hep-ex/9805026].
- [12] Y. Inoue, T. Namba, S. Moriyama, M. Minowa, Y. Takasu, T. Horiuchi and A. Yamamoto, Phys. Lett. B **536** (2002) 18 [astro-ph/0204388].

- [13] Y. Inoue, Y. Akimoto, R. Ohta, T. Mizumoto, A. Yamamoto and M. Minowa, *Phys. Lett. B* **668** (2008) 93 [arXiv:0806.2230].
- [14] S. Chang and K. Choi, *Phys. Lett. B* **316** (1993) 51 [hep-ph/9306216].
- [15] Z. G. Berezhiani, A. S. Sakharov and M. Y. Khlopov, *Sov. J. Nucl. Phys.* **55** (1992) 1063 [*Yad. Fiz.* **55** (1992) 1918].
- [16] K. Ichikawa, M. Fukugita and M. Kawasaki, *Phys. Rev. D* **71** (2005) 043001 [astro-ph/0409768].
- [17] D. Larson *et al.*, arXiv:1001.4635.
- [18] E. Komatsu *et al.*, arXiv:1001.4538.
- [19] C. L. Reichardt *et al.*, *Astrophys. J.* **694** (2009) 1200 [arXiv:0801.1491].
- [20] H. C. Chiang *et al.*, arXiv:0906.1181.
- [21] M. L. Brown *et al.* (QUaD collaboration), *Astrophys. J.* **705** (2009) 978 [arXiv:0906.1003].
- [22] B. A. Reid *et al.*, arXiv:0907.1659.
- [23] J. Hamann, S. Hannestad, J. Lesgourgues, C. Rampf and Y. Y. Y. Wong, arXiv:1003.3999.
- [24] W. J. Percival *et al.*, *Mon. Not. Roy. Astron. Soc.* **401** (2010) 2148 [arXiv:0907.1660].
- [25] A. G. Riess *et al.*, *Astrophys. J.* **699** (2009) 539 [arXiv:0905.0695].
- [26] A. Lewis and S. Bridle, *Phys. Rev. D* **66** (2002) 103511 [astro-ph/0205436].
- [27] F. De Bernardis, T. D. Kitching, A. Heavens and A. Melchiorri, *Phys. Rev. D* **80** (2009) 123509 [arXiv:0907.1917].
- [28] J. Lesgourgues and S. Pastor, *Phys. Rept.* **429** (2006) 307 [astro-ph/0603494].
- [29] D. Grin, T. L. Smith and M. Kamionkowski, *Phys. Rev. D* **77** (2008) 085020 [arXiv:0711.1352].
- [30] E. J. Chun, D. Comelli and D. H. Lyth, *Phys. Rev. D* **62** (2000) 095013 [hep-ph/0008133].